BIOCHEMISTRY
including biophysical chemistry & molecular biology

Accelerated Publication

pubs.acs.org/biochemistry

Reconstructing a Missing Link in the Evolution of a Recently Diverged Phosphotriesterase by Active-Site Loop Remodeling

Livnat Afriat-Jurnou,[†] Colin J. Jackson,[‡] and Dan S. Tawfik*,[†]

[†]Department of Biological Chemistry, The Weizmann Institute of Science, Rehovot 76100, Israel

[‡]Research School of Chemistry, The Australian National University, 0200, Australian Capital Territory, Australia

Supporting Information

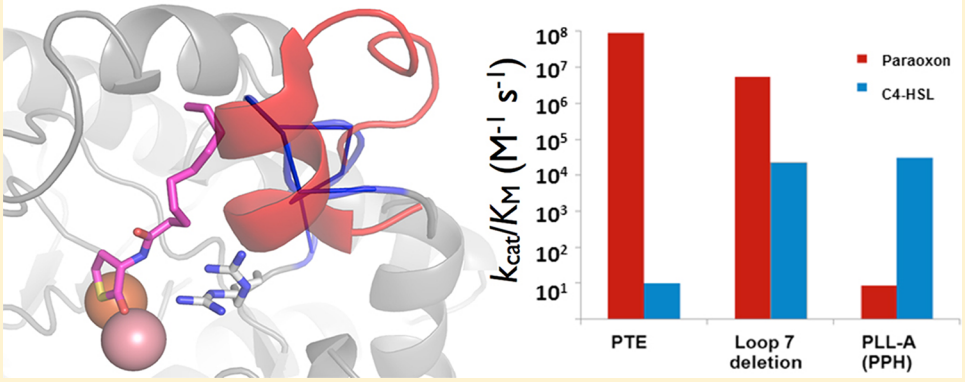

ABSTRACT: Only decades after the introduction of organophosphate pesticides, bacterial phosphotriesterases (PTEs) have evolved to catalyze their degradation with remarkable efficiency. Their closest known relatives, lactonases, with promiscuous phosphotriasterase activity, dubbed PTE-like lactonases (PLLs), share only 30% sequence identity and also differ in the configuration of their active-site loops. PTE was therefore presumed to have evolved from a yet unknown PLL whose primary activity was the hydrolysis of quorum sensing homoserine lactones (HSLs) (Afriat et al. (2006) *Biochemistry 45*, 13677−13686). However, how PTEs diverged from this presumed PLL remains a mystery. In this study we investigated loop remodeling as a means of reconstructing a homoserine lactonase ancestor that relates to PTE by few mutational steps. Although, in nature, loop remodeling is a common mechanism of divergence of enzymatic functions, reproducing this process in the laboratory is a challenge. Structural and phylogenetic analyses enabled us to remodel one of PTE's active-site loops into a PLL-like configuration. A deletion in loop 7, combined with an adjacent, highly epistatic, point mutation led to the emergence of an HSLase activity that is undetectable in PTE (k_{cat}/K_M values of up to 2×10^4). The appearance of the HSLase activity was accompanied by only a minor decrease in PTE's paraoxonase activity. This specificity change demonstrates the potential role of bifunctional intermediates in the divergence of new enzymatic functions and highlights the critical contribution of loop remodeling to the rapid divergence of new enzyme functions.

The enzyme now known as phosphotriesterase (PTE) was first observed in the 1980s in soil bacteria isolated from sites contaminated with parathion, the first widely used organophosphate pesticide, and paraoxon, its oxidation product that comprises the actual pesticide (Figure 2).[1] Although organophosphates were widely introduced only in the 1950s, PTE has rapidly evolved to catalyze the hydrolysis of these synthetic compounds with rates approaching the diffusion limit ($k_{cat}/K_M \sim 10^8$ M^{-1} s^{-1} with paraoxon).[2] PTE's evolutionary history remains a mystery — how could a new enzymatic activity emerge so rapidly towards a synthetic substrate with no natural analogues?[3] It has been proposed that new enzymes originate from coincidental, promiscuous, activities of existing enzymes.[4,5] Such promiscuous activities could endow the organism with an initial selective advantage — a new phosphate source in PTE's case, and subsequently evolve via mutations and selection to give a specialized, proficient enzyme. A recent work on the emergence of insecticide resistance via bacteria−insect symbiosis[6] supports the notion that PTE's evolution is connected to insecticide resistance. The utilization of organophosphates as a phosphorous source comprises another potential driving force.[7]

In conjunction with this hypothesis, we identified a family of lactonases that belong to the same amidohydrolase superfamily as PTE.[8] Members of this family named PTE-like lactonases (PLLs) hydrolyze lactones, including homoserine lactones (HSLs) that serve as bacterial quorum-sensing signals.[9] All known PLLs exhibit promiscuous phosphotriesterase activity.[9−14] Conversely, PTE exhibits a weak, promiscuous lactonase activity that could be a vestige of its PLL ancestor.[9,15]

Received: May 27, 2012
Published: July 18, 2012

   dx.doi.org/10.1021/bi300694t | *Biochemistry* 2012, 51, 6047−6055

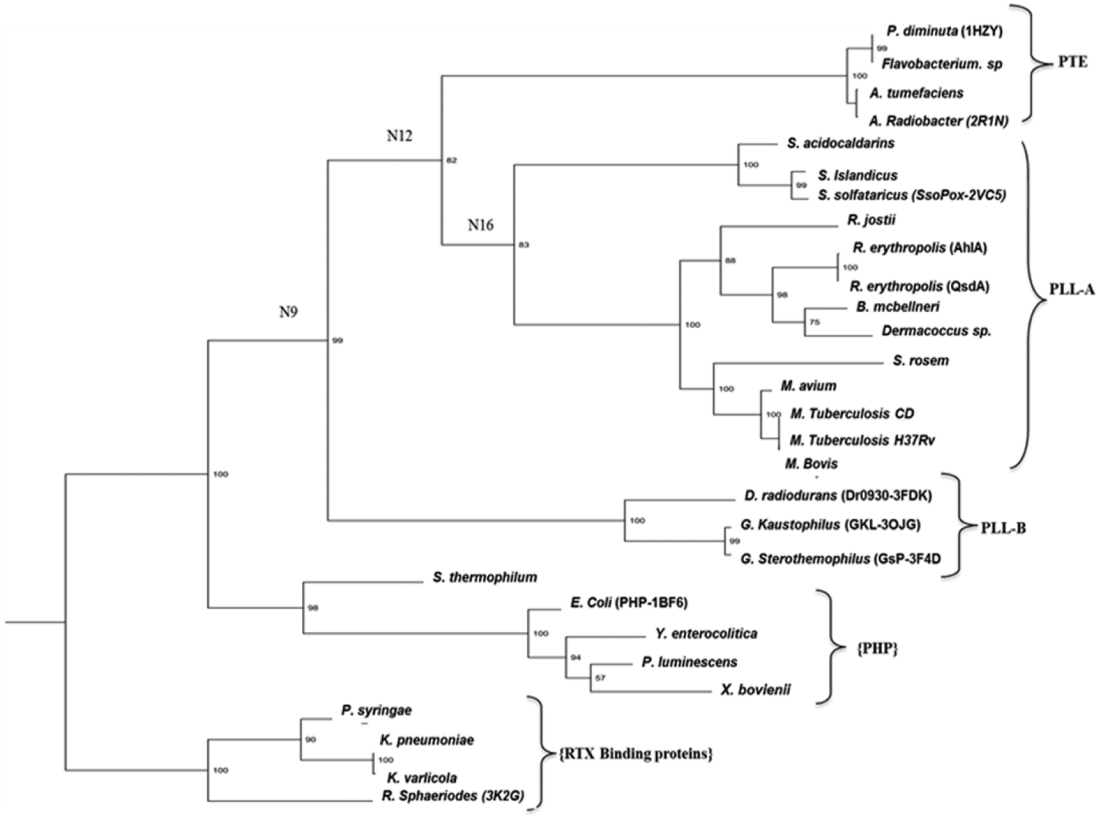

Figure 1. A phylogenetic tree of PTE and related families. The tree was calculated using the PhyML program with the LG substitution matrix and gamma distribution. The tree consisted of three distinct clades: PTEs and two lactonase clades that we dubbed as PLL-A and PLL-B. Marked in brackets are the outgroup families used, PHP, and RTX binding protein. Although their enzymatic specificity remains unknown, PTE homology proteins (PHPs)[31] and RTX binding proteins (resiniferatoxin-binding, phosphotriesterase-related proteins[38]) appear in numerous organisms including bacteria and mammals. They relate to PTE, both in structure and sequence, and possess unique configurations of active-site loops (Figure S1). The bootstrap analysis values derived from 100 individual runs are indicated at each node. Ancestral predictions were obtained for the common ancestors of PTE and the PLLs (N9, N12, N16).

The notion that PTE's progenitor is an as yet unknown PLL member is supported by the shared TIM-barrel fold and essentially identical bimetallo catalytic centers.[9,16] The lactonase ancestor hypothesis is hampered, however, by the fact that known PLLs only share ~30% sequence identity with PTE. Besides >200 substitutions, there are also length differences in most active site loops, particularly in loop 7 which is 14 amino acids longer in PTE (loops are numbered by the α/β modules of the TIM-barrel fold). Thus, an evolutionary link between PLLs and PTE, namely, a PLL with more obvious sequence, structure, and activity homology to PTE, is crucially missing. Such a missing link could be discovered (because PTE diverged so recently) but can also be reconstructed using a combination of phylogenetic and protein engineering.[17]

Reconstruction, however, should address not only the function-altering substitutions (side-chain replacements) but also backbone length modifications driven by insertions and deletions (InDels). The latter often drive the acquisition of new protein functions.[18−20] In particular, "loop remodeling", that is, changes in length and configuration of active-site loops, is thought to play a key role in the divergence of enzyme functions.[21,22] Indeed, in enzyme superfamilies, including the amidohydrolase superfamily to which PTEs and PLLs belong,[8] the overall structural fold and key active site residues are conserved, whereas the length, sequence, and structural conformation of certain active-site loops is highly variable.[22,23] However, although common in nature, the laboratory remodeling of active-site loops remains a challenge for rational design, directed evolution, or computational design.[10,11,13,14,24−28] In contrast to numerous examples of functional transitions via point mutations, only a few successful examples of loop remodeling have been reported. These demanded extensive and simultaneous sequence changes, which are unlikely to occur in nature, and have typically resulted in enzymes whose catalytic activities are low.[11,24−28] Conversely, remodeling of the active-site loops of PLLs by exchange with PTE's loop(s) resulted in nonfunctional proteins.[9−12,14] To test the hypothesis that PTE have evolved from an unknown PLL member, we have remodeled PTE's active-site loop 7 and thereby restored the ancestral lactonase activity.

EXPERIMENTAL PROCEDURES

Alignments, Phylogenetic Tree, and Ancestral Reconstruction. Sequences of PTE-related proteins were collected from the NCBI nonredundant protein sequence database (nr) using protein-alignment BLAST (blastp) with default settings. The multiple sequence alignment presented in this work was created with MUSCLE.[29] As different alignment programs assigned different gaps in the active-site loops, the alignment was manually refined using the structures of PTE and related enzymes (PDB codes: 1HZY[30] (PTE from *Pseudomonas Diminuta*), 2VC7[16] (SsoPox from *Sulfolobus solfataricus*), 3FDK[10] (Dr0930 from *Deinococcus radiodurans*), 1BF6[31] (PHP from *Escherichia coli*), and 3K2G (resiniferatoxin binding

dx.doi.org/10.1021/bi300694t | *Biochemistry* 2012, 51, 6047−6055

protein from *Rhodobacter sphaeroid*). The optimal evolutionary model (LG + I + G) was obtained by ProtTest.[32] The phylogenetic tree was calculated using PhyML program with the LG substitution matrix and gamma distribution. The bootstrap resample test was performed 100 times to confirm the tree's reliability. Sequence predictions for the ancestral nodes of PTE and the PLLs (Figure 1) were obtained with FastML.[33] The design of the ancestral library was based on the most probable ancestral sequence of node N12 (Figure S7), using the principles described in ref 34.

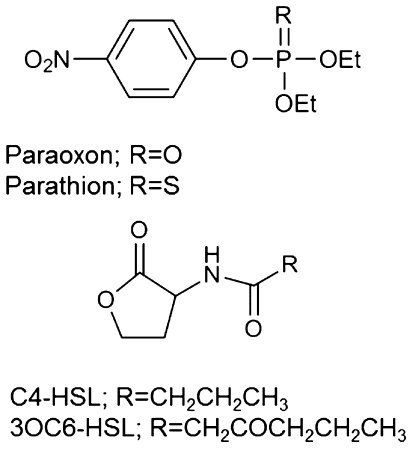

Figure 2. Structures of PTE's and PLL's substrates. Paraoxon (R = O) and parathion (R = S) comprise the substrates for which PTE is thought to have evolved. The presumed native substrates of PTE-like lactonases (PLLs) are primarily homoserine lactones (HSLs). HSLs are named in accordance to their N-acyl groups, which can be simple alkyl chains of variable lengths (e.g., C4-HSL, correspond to *N*-(butyryl) homoserine lactone), or 3-oxo-alkyl chains (e.g., 3OC6-HSL, correspond to *N*-(3-oxohexanoyl) homoserine lactone). δ-Lactones, and γ-lactones other than HSLs, are also substrates of PLLs (primarily of the PPL-B clade).

Construction of PTE Variants. PTE-S5, a highly expressing variant of *P. diminuta* PTE with three surface mutations and wild-type-like kinetic parameters,[35] was used as a starting point for PTE designs. The deletion and single point mutants were constructed by blunt-end mutagenesis. The amplified gene of PTE-S5, and its variants, were fused to the C-terminus of maltose binding protein (MBP) gene by cloning into pMAL-c2x (NEB) using *Eco*RI and *Pst*I restriction sites.[35] The ligated plasmids were electroporated to *E. coli* DH5α. DNA sequencing validated the constructs, and the plasmids were transformed to *E. coli* BL21 cells for expression.

Libraries Construction and Directed Evolution Experiments. Libraries were constructed using the incorporating synthetic oligos via gene reassembly (ISOR) protocol for generating random combinations of specific mutations.[36] The resulting assembly reaction was followed by a nested PCR with external primers, digestion with *Eco*RI and *Pst*I, ligation into pMAL-c2x, electroporation into *E. coli* DH5α, and isolation of plasmid DNA.

Libraries Screen. Plasmids were transformed into BL21 cells, plated on LB agar with 100 μg/mL ampicillin, and 400–800 randomly picked single colonies were grown overnight in 96 deep-well plates, at 30 °C with shaking, in LB medium with 100 μg/mL ampicillin. These were used to inoculate (at 1:20 dilution) fresh LB medium with 100 μg/mL ampicillin and 0.5 mM $ZnCl_2$, in 96 deep-well plates. Cells were grown at 30 °C with shaking to OD_{600} = 0.6–1.0 (~4 h) and 0.4 mM IPTG was added to induce overexpression. Following overnight growth, the cells were pelleted and stored at −80 °C. Cells were lysed as described in ref 9. The lysates were clarified by centrifugation, diluted according to the level of activity, and assayed in 200 μL reactions for the hydrolysis of 0.25 mM TBBL and 0.25 mM paraoxon.

Expression and Purification. LB medium (5 mL) containing 100 μg/mL ampicillin and 0.5 mM $ZnCl_2$ was inoculated with a single colony of freshly transformed *E. coli* BL21, and grown overnight at 30 °C. Inoculates were added to 500 mL of LB with 100 μg/mL ampicillin and 0.5 mM $ZnCl_2$ and grown at 30 °C to $OD_{600\ nm} \approx 0.6$, isopropyl-beta-D-thiogalactopyranoside (IPTG) was added (0.4 mM) and cultures were grown overnight. Cells were harvested by centrifugation and resuspended with 25 mL BugBuster HT Protein Extraction Reagent (Novagen), 10 mM $NaHCO_3$, 1:500 dilution of protease inhibitor cocktail (Sigma), and 100 μM $ZnCl_2$. The clarified lysate was passed through an amylose column (NEB) equilibrated with buffer A (100 mM Tris pH 8.0, 0.25 M NaCl and 100 μM $ZnCl_2$). The MBP–PTE fusion protein was eluted with column buffer supplemented with 10 mM maltose. Enzyme containing fractions were pooled and dialyzed at 4 °C against activity buffer A. Purity and protein concentrations were examined by 12% SDS–PAGE and by absorbance at 280 nm (extinction coefficient values for the MBP fused enzymes were calculated with ProtParam (http://web.expasy.org/protparam).

Enzyme Kinetics. Hydrolysis rates were determined at 25 °C (pH 8.0 in the case of paraoxon and TBBL) by monitoring absorbance changes in 200 μL reactions using 96-well plates and a microtiter plate reader (Synergy HT; optical length ~0.5 cm). Substrates were dissolved in acetonitrile, and the final organic solvent concentration was maintained at ≤1%. The monitoring wavelength, and the product's extinction coefficient, were 405 nm, ε = 9500 OD/M, for paraoxon; TBBL, together with 0.5 mM 5,5′-dithiobis(2-nitrobenzoic acid) (DTNB) as indicator, 412 nm, ε = 7000 OD/M. The hydrolysis of HSLs was monitored by following the appearance of their carboxylic acid products using the pH-indicator assay, as previously described in ref 9. The reactions contained 0.01–1 mM of the HSL substrate (dissolved in DMSO) in 2.5 mM bicine buffer pH 8.3 supplemented with 0.2 M NaCl and 0.2–0.3 mM cresol purple as pH indicator. Rates were monitored at 577 nm, based on extinction coefficients determined with acetic acid calibration curve within the same run (ε = 1550–2700 OD/M). Initial rates (v_0) were corrected for the background rate of spontaneous hydrolysis in the absence of enzyme. Kinetic parameters were obtained by fitting initial rates directly to the Michaelis–Menten equation $[v_0 = k_{cat}[E]_0[S]_0/([S]_0 + K_M)]$ with the softwares GraphPad Prism or Kaleidagraph. Error ranges relate to the standard deviation of the data obtained from three independent measurements, or to the actual difference between measurements in cases of two measurements.

Structural Modeling. The model of PTE with bound substrate was generated by superposing the structure of PTE from *P. diminuta* (1HZY)[30] with the substrate bound (diethyl 4-methoxyphenyl phosphate) structure of PTE from *Agrobacterium radiobacter* (2R1N)[37] (Figure 3b). The model of PTE with bound HSL (Figure 3c) was generated by superposition of SsoPox's structure with a C10-HSL analogue (PDB: 2VC7).[16] The model of SsoPox with paraoxon (2d) was derived by

dx.doi.org/10.1021/bi300694t | *Biochemistry* 2012, 51, 6047–6055

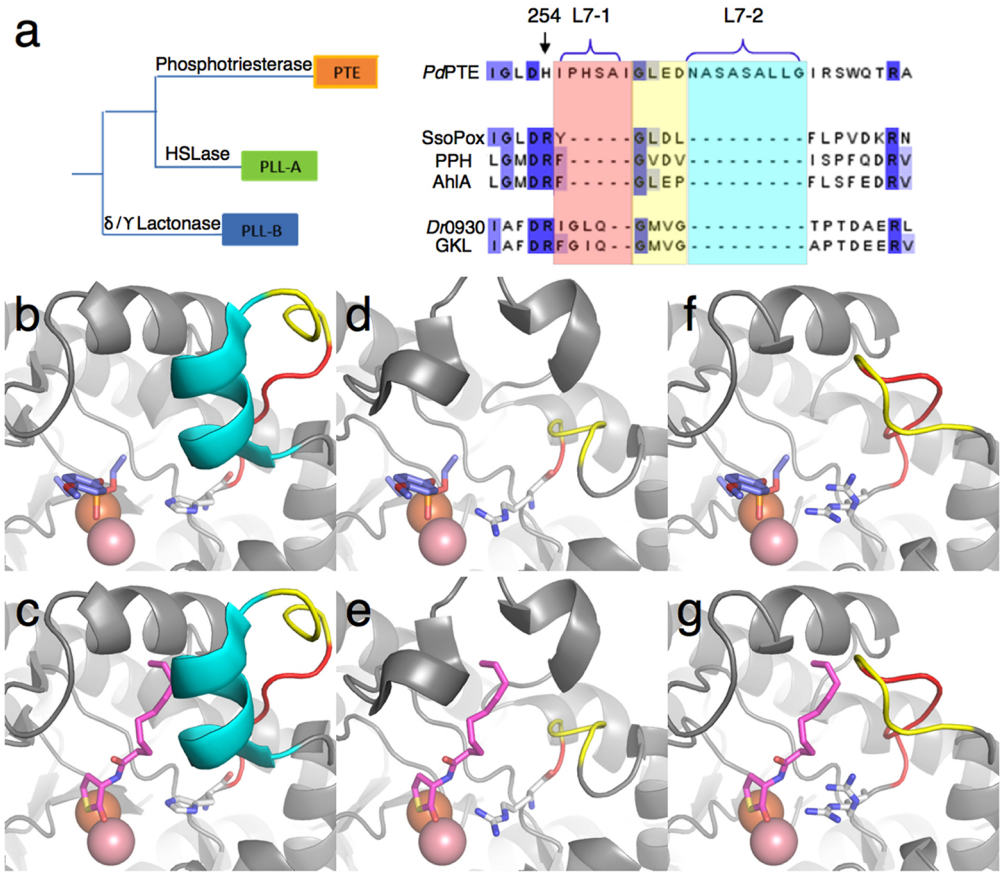

Figure 3. The active-site loop 7 of PTE, of SsoPox (a lactonase from the PLL-A clade), and of a model of the engineered PTEΔ7-2/254R. (a) Refined sequence alignment of Loop 7 region of PTE, PLL-As (SsoPox, PPH, and AhlA), and PLL-Bs (Dr0930 and GKL). The alignment is color coded with the two segments of loop 7 (L7-1 and L7-2), and the connecting anchor (yellow). The same color scheme is used in the structures presented in the lower part. (b) PTE's active site is complementary to paraoxon as indicated by the structure of its complex with a paraoxon analogue (blue sticks). (c) Binding of HSLs to PTE, particularly with long acyl chains (e.g., C12-HSL, magenta sticks), is blocked by the L7-2 segment. Catalysis of lactone hydrolysis is also impeded by having His at position 254 (in sticks, next to the two catalytic metals). SsoPox's active site is widely open for paraoxon (d), and complementary to HSLs with long acyl chains (e); note the positioning of R223, the match of PTE's H254, against the lactone's ester group). (f) The structural modeling of PTEΔ7-2/254R (PTE with the H254R mutation and the L7-2 segment deleted) indicates an intermediate loop configuration between PTE and SsoPox. This configuration seems to accommodate paraoxon (f) as well as long chain HSLs (g). The generation of these models is described in the Experimental Procedures.

superposition of PTE with a paraoxon analogue (2R1N). The structural model of PTEΔ7-2/254R was generated using the Swiss-Model workspace (http://swissmodel.expasy.org). The model was of high quality, with an above average QMEAN Z-score for a protein of its size (0.84). The essentially identical structure of PTE from *A. radiobacter* that has Arg at 254 (2R1N) was used to model the Arg side chain in PTEΔ7-2/254R (Figure 3f,g).

RESULTS

Comparative Analysis of PTEs and PLLs. A phylogenetic tree of PTE and its closest related sequences was constructed based on the multiple sequence alignment (Figure 1, Figure S1). The tree contains two outgroups: PTE homology proteins (PHPs)[31] and RTX binding proteins (resiniferatoxin-binding, phosphotriesterase-related proteins).[38] The tree also contains three clades which are more closely related: PTEs and two lactonase clades that we dubbed as PLL-A and PLL-B. These three clades exhibit distinct enzymatic specificities as described below. Although the tree reconstruction algorithm does not take into account insertions and deletions (gaps, at the alignment level), the three clades also show distinct active-site loops configurations (Figure 3a). Most notably, PTE's loop 7 is 14 amino acids longer than in PLL-As (7), and 11 amino acids longer than PLL-Bs. Functionally, the characterized members of the PLL-A clade such as SsoPox,[16] PPH and AhlA,[9] and MCP,[11] are quorum-quenching lactonases. These enzymes specialize in hydrolyzing HSLs with different N-acyl chains (Figure 2) but may also hydrolyze other γ- or even δ-lactones. PPH and AhlA's best substrate is 3OC8-HSL (k_{cat}/K_M values of ~10^5 M^{-1} s^{-1}) (7). MCP only hydrolyzes HSLs with alkyl N-acyl chains (i.e., without the 3-oxo group),[11] for example, C12-HSL with k_{cat}/K_M of ~10^4 M^{-1} s^{-1}. In contrast, enzymes belonging to the PPL-B clade, represented by the biochemically characterized Dr0930,[10,14] GsP,[13] and GKL,[12] exhibit no, or weak activity with HSLs, and hydrolyze other γ- or δ-lactones with k_{cat}/K_M values up to 10^5 M^{-1} s^{-1}. Besides their lactonase activities, all known PLLs from both clades exhibit promiscuous phosphotriesterase activity,[9−12,14,16,39] with SsoPox being the most active (k_{cat}/K_M ~ 10^3 M^{-1} s^{-1}).[16,39,40]

Although identified in geographically distant locations,[41] the known phosphotriesterase variants - PTE from *P. diminuta*[1] and *Flavobacterium sp.*,[42] and OpdA from *A. tumefaciens* and *A. radiobacter*,[43] show ≥90% amino acid sequence identity and

dx.doi.org/10.1021/bi300694t | *Biochemistry* 2012, 51, 6047−6055

Table 1. Kinetic Parameters for the Paraoxonase and Lactonase Activities of Different PTE Variants

		PTE[a] (254H)	PTE 254R	PTE Δ7-1/254R	PTE Δ7-2(254H)	PTE Δ7-2/254R	PTE Δ7-1 + 2[b]	PTE Δ7-2/1-3B[c]
paraoxon	K_M (μM)	48 ± 6	27 ± 3	424 ± 108	690 ± 130	430 ± 60	312 ± 78	2800 ± 780
	k_{cat} (s^{-1})	4361 ± 163	410 ± 20	45 ± 5	1490 ± 108	2319 ± 84	2.4 ± 0.2	0.26 ± 0.04
	K_{cat}/K_M (M^{-1} s^{-1})	9.08×10^7	1.52×10^7	1.06 x10^5	2.1×10^6	5.4×10^6	7.7×10^3	93
TBBL	K_M (μM)	260 ± 3	720 ± 312	780 ± 150	210 ± 40	1066 ± 19	1000 ± 140	1840 ± 450
	k_{cat} (s^{-1})	0.90 ± 0.04	3.7 ± 0.2	0.93 ± 0.05	0.26 ± 0.92	24 ± 2	0.05 ± 0.002	42.7 ± 4.6
	K_{cat}/K_M (M^{-1} s^{-1})	3460	5180	1190	1240	2.26×10^4	53	2.3×10^4
C4-HSL	K_M (μM)			185 ± 45		63 ± 20	184 ± 45	204 ± 24
	k_{cat} (s^{-1})			0.07 ± 0.01		1.3 ± 0.1	0.20 ± 0.02	0.74 ± 0.04
	K_{cat}/K_M (M^{-1} s^{-1})	≤9.5[d]	≤9.5	378	≤9.5	2.2×10^4	1090	3.7×10^3
3OC6-HSL	K_M (μM)					880 ± 185	360 ± 130	
	k_{cat} (s^{-1})					4.3 ± 0.4	0.11 ± 0.02	
	K_{cat}/K_M (M^{-1} s^{-1})	≤3.5[d]	≤3.5	≤3.5	≤3.5	4900	300	≤3.5

[a]Variants described here were all based on a recombinant variant of PTE dubbed PTE-S5 that exhibits high soluble expression level in *E. coli* and essentially the same kinetic parameters as wild-type PTE; this variant carries three mutations at surface positions away from the active site.[35] [b]Both segments of loop 7 were deleted in this variant that also carries the following point mutations: H254R, I255Y, D264V, and R275L. [c]Segment L7-2 was deleted in this variant that also carries the following point mutations: G60 V, F132Y, H254R, M317L, and I284 V. [d]No activity above the spontaneous, background rate of hydrolysis could be detected at the highest enzyme concentration applied (2.25 μM). For C4-HSL, this detection limit corresponds to k_{cat}/K_M = 9.5 M^{-1} s^{-1}, and for 3OC6-HSL the limit is 3.5 M^{-1} s^{-1}.

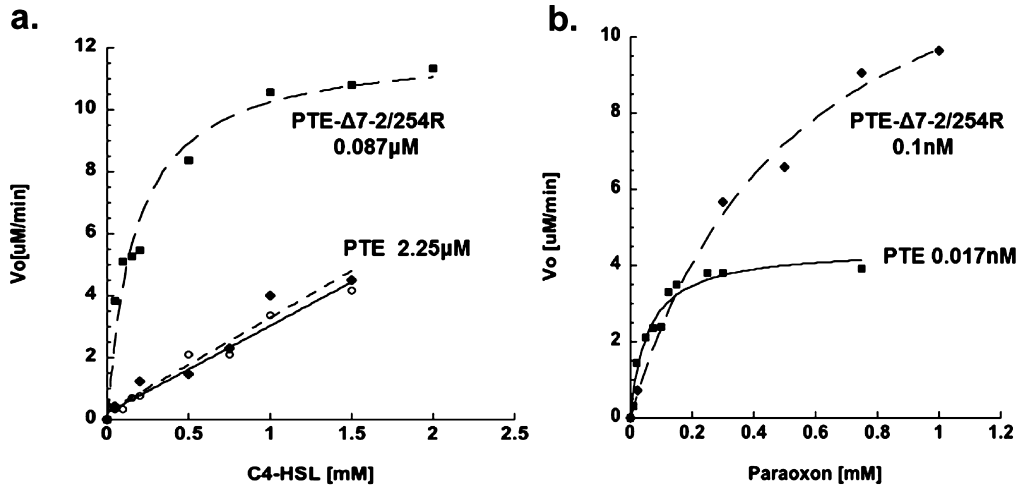

Figure 4. Michaelis–Menten plots for the HSLase and paraoxonase activity of PTE and PTEΔ7-2/254R. (a) HSLase activity assayed at pH 8.0, 25 °C, with C4-HSL and enzyme variants PTE-S5 ($[E]_0$ = 2.25 μM) and PTEΔ7-2/H254R ($[E]_0$ = 0.087 nM). The spontaneous, background rate of hydrolysis could be detected at the highest enzyme concentration applied (2 μM); this detection limit corresponds to k_{cat}/K_M = 9.5 M^{-1} s^{-1} (○). (b) The paraoxonase activity assayed under the same conditions with PTE-S5 ($[E]_0$ = 0.017 nM) and PTE-Δ7-2/H254R ($[E]_0$ = 0.1 nM).

have probably diverged from a very recent common ancestor. These PTEs are highly efficient phosphotriesterases (k_{cat}/K_M > 10^7 M^{-1} s^{-1} for paraoxon, parathion, and/or their methyl analogues).[2,44] They also exhibit weak, promiscuous, lactonase activity with an aromatic lactone,[15] and with a synthetic chromogenic lactone dubbed 5-thiobutyl-γ-butyrolactone (TBBL).[9] However, we detected no rate acceleration by PTE with γ- or δ-lactones (the best substrates of PLL-Bs). We also failed to detect rate enhancement with HSLs, although the high background rate of the lactonase assays sets a relatively low detection threshold (k_{cat}/K_M = 3.5–9.5 M^{-1} s^{-1}; Table 1).

Loop 7's Configuration Determines Substrate Specificity. Structural analysis indicated that the lack of homoserine lactonase (HSLase) activity seems to relate to the reshaping of PTE's active site by the 14-amino-acid insertion in loop 7 (Figure 3). This long loop plays a role in substrate binding and product release by PTE.[45] We therefore aimed to truncate PTE's loop 7 assuming that this will endow the enzyme with its ancestral HSLase activity. This, however, proved to be far from trivial. Standard alignment algorithms assigned a single 14-amino-acid insertion in PTE (Figure S3), both in our hands and in others.[7−11] However, deletion of this 14-amino-acid stretch resulted in a soluble but completely inactive protein. Parallel attempts to transplant PTE's loop 7 along with loop 8, or all eight active-site loops, into various PLLs resulted in an insoluble, or inactive, proteins.[10,11] Further examination of the sequence and structure alignments indicated that the 14-amino-acid insertion in PTE's loop 7 actually consists of two individual insertions events separated by a 4-amino-acid spacer (annotated as L7-1 and L7-2, Figure 3a). The spacer includes Gly261, which is conserved throughout PLLs and PTEs (all residue numbers refer to PTE's sequence). Structural alignment of PTE and GsP[13] (a PLL-B) also indicated that Gly232 at the N-terminus of GsP's loop 7 superposes with Pro256 in PTE (Figure S4). The additional three amino acids in loop 7 of PLL-Bs were therefore aligned with PTE's L7-1 segment (Figure 3a). The two loop 7 segments differ in their structural features. Compared to L7-1, the L7-2 segment is solvent exposed,

dx.doi.org/10.1021/bi300694t | *Biochemistry* 2012, 51, 6047−6055

loosely packed, and exhibits fewer interactions with the rest of PTE's structure. The average solvent accessibility value for the L7-1 residues is 0.05 (a value assigned to highly buried core residues) versus 0.19 for L7-2. The average number of contacts per residue is 5.5 for L7-2 versus 9.3 for L7-1. In accordance, the L7-2 segment shows higher flexibility (average B-factor 22.6 Å^2 versus 16.8 Å^2 for L7-1 segment; Figure S5). These structural features, and the alignment of PTE with PLL-As versus PLL-Bs, suggested that these two parts of loop 7 could diverge independently from one another. Given its loose connections to the rest of PTE's structure, and its absence in both PLL-As and PLL-Bs, the L7-2 insertion is much more likely to have been the most recent loop remodeling event in the divergence of PTEs. Structural modeling indicated that, as expected, truncation of L7-2 results in an intermediate loop configuration between PTE and PLL-A. This suggested that the deletion of this segment alone might be sufficient to remove the blockage of access to HSLs imposed by PTE's long loop 7 (especially to long acyl chain HSLs; Figure 3b–g).

Reverting Loop 7-2 Insertion Turns PTE into a Bifunctional Enzyme. In contrast to the single 14-amino-acid loop 7 deletion, individual deletions of each of the two segments gave active enzyme variants (the deletion mutants are dubbed PTEΔ7-1 (P256–I260 deleted) and PTEΔ7-2 (N265–G273 deleted); Figure 3a). However, as discussed below, the effect of these loop 7 deletions was entirely dependent on a single point mutation of His to Arg in loop 7 at position 254. The results described below therefore refer to deletions made in the background of the H254R mutant of PTE. The designed variant with segment L7-1 deleted (PTEΔ7-1/254R) showed a ∼1000-fold decrease in the paraoxonase activity and an increase in the hydrolysis of C4-HSL from a nondetectable level in PTE to k_{cat}/K_M of ∼400 M^{-1} s^{-1} (Table 1). The deletion of the second segment (PTEΔ7-2/254R) resulted in ≥2000-fold increase in the HSLase activity to a k_{cat}/K_M value of ∼10^4 M^{-1} s^{-1} with both C4-HSL and 3OC6-HSL (Figure 4a). Remarkably, the L7-2 deletion led to only a 17-fold reduction in the paraoxonase activity, primarily via an increase in K_M (Figure 4b). These results are in agreement with the insertion of the L7-2 segment being the last loop-remodeling event in PTE's evolution. The deletion variant PTEΔ7-2 (in the background of H254R) is therefore a bifunctional intermediate exhibiting high paraoxonase activity alongside moderately high HSLase activity (Figure 4). This laboratory reversion of PTE into a PLL-like enzyme provides a better understanding regarding how, starting from a PLL member with a similar loop configuration as our engineered intermediate, the insertion of the L7-2 loop segment, and the following point mutation R254H, could have led to a paraoxonase activity at a near-diffusion-rate while effectively erasing the progenitor's HSLase activity.

The Epistatic Effect of Position 254. In the background of wild-type PTE, the L7-2 deletion had almost no effect on the lactonase activity (Table 1; PTEΔ7-2/254H). We therefore assumed that this insertion must have occurred in the background of other amino acid substitutions. Although these point mutations cannot be easily distinguished at a level of 70% divergence, the mutation H254R at the N-terminus of loop 7 (Figure 3a) was an obvious suspect. This position is connected to loop 7 through backbone hydrogen bonds.[45] The corresponding residue of Arg254 in PLLs (Arg 223 in SsoPox) plays a role in stabilizing the oxyanionic intermediate of lactone hydrolysis (Figure S6). The H254R mutation also appeared in directed evolution experiments aimed to increase PTE's promiscuous aryl-esterase activity[35] (note that lactones are cyclic esters). Indeed, whereas in wild-type PTE, the L7-2 deletion had no significant effect on lactonase activity, in the 254R background, the L7-2 deletion induced a relatively high level of HSLase activity (Table 1).

H254R is therefore a striking example of a highly epistatic mutation upon which the reversion of loop 7-2's insertion depends. The R254H mutation most likely occurred as one of the final steps in PTE's divergence, and only in two out of the four known PTEs (including *P. diminuta*). All PLLs, and the predicted common ancestor of PTEs and PLL-As (N12), have Arg at position 254 (Figure S7). Indeed, the R254H mutation yielded only a slight increase in the turnover rate in an enzyme that was already highly efficient (∼4-fold; Table 1). However, once this position changed to His, it acted as an epistatic ratchet,[46] blocking the ability of PTE to revert into the bifunctional HSLase-PTE intermediate, from which it presumably diverged.

Further Steps beyond Loop 7-2 Deletion. Assuming that the deletion variant PTEΔ7-2/254R can represent a very recent intermediate along PTE's evolutionary trajectory, we asked whether earlier intermediates can be reconstructed? Such attempts are hampered by two factors: first, the H254R mutation and the L7-2 deletion stood out as recent mutational events, but the sequence of earlier intermediates cannot be as easily inferred (the currently known PLLs are ∼70% diverged from PTE). Poor inference capabilities can be bridged by combinatorial, library explorations. However, the HSLase activity with C4-HSL and 3OC6-HSL could only be assayed with purified enzyme variants. Library screens were therefore limited to the chromogenic lactone TBBL and paraoxon. Within these limitations, we explored additional changes within loop 7 as well as in other active-site loops. We sought variants that may resemble earlier intermediates by virtue of exhibiting lower phosphotriesterase activity and/or higher lactonase activity relative to PTEΔ7-2/254R.

We first attempted to produce an enzyme with a similar loop configuration to PLL-As by deleting both segments of loop 7. Assuming that, as is the case with H254R, point mutations may render this double-deletion variant functional, mutation to the corresponding PLL-A residues at various positions flanking the two loop 7 segments were combinatorially introduced (I255F/Y, L262 V, E263D, D264 V/L/P, and R275L/S; Figure 3a). The resulting library (constructed after deletion of L7-1 and L7-2) was screened for active variants. The best variant identified exhibited >1000-fold lower paraoxonase activity than that of PTE (k_{cat}/K_M ∼ 8 × 10^3 M^{-1} s^{-1}; see PTEΔ7-1 + 2 in Table 1). It exhibited considerable HSLase activity (k_{cat}/K_M 2 × 10^3 M^{-1} s^{-1} with C4-HSL), albeit ∼10-fold lower than PTEΔ7-2/254R (Table 1).

We also attempted to identify other substitutions that correlate with loop 7-2 deletion (in addition to H254R) that may therefore underline earlier intermediates. We compared PTE's sequence to the predicted sequences of the ancestral nodes connecting PTEs and PLL-A (Figure S7). This enabled us to identify substitutions that occurred along PTE's divergence within and near its active site. These were combinatorially incorporated into PTEΔ7-2/254R to give a so-called ancestral library[34] (Table S2). Screening identified several variants that exhibited up to 10^6-fold reversals in enzymatic specificity: from a TBBL/paraoxon ratio of ∼3 × 10^{-5} in wild-type PTE, to ∼250 in PTEΔ7-2/1-3B (Table 1).

However, this reversal was mostly driven by a drastic decline in the paraoxonase activity (>10^5-fold lower than PTE's), whereas the HSLase activity was ~5 fold lower than PTEΔ7-2/254R. Nonetheless, these variants included mutations in active-site loops 1, 3, and 8 that appear to have been crucial to the emergence of PTE's paraoxonase activity. For example, tyrosines at active-site positions 131 and 132 (loop 3) seem to be a hallmark of PLL's active sites, whereas Trp and Phe are found in these positions in PTE.[7,10,11,16] Accordingly, the ancestral substitutions W131Y and F132Y were individually observed in selected variants.

DISCUSSION

Although artificially engineered in the laboratory, the reconstructed PTEΔ7-2/254R variant is likely to represent the key features of the actual intermediate on the trajectory that connected PTE and its presumed PLL ancestor. These key features are loop 7's configuration and the dual HSLase–paraoxonase enzyme function. This assumption is supported by the following observations: (i) 254Arg (and not His) comprises the most likely ancestral state, so in effect, the reproduced deletion variant is linked through one mutational step — a deletion in loop 7. (ii) The loop 7-2 segment is largely detached from the rest of the enzyme (Figure 3), suggesting that it comprises a recent insertion. (iii) Its deletion caused no major destabilization or disruption of the active-site (and so would its insertion in the actual trajectory). (iv) The bifunctional activity profile of PTEΔ7-2/254R is compatible with the expected properties of an evolutionary intermediate along a trajectory leading from an HSL with a promiscuous phosphotriesterase activity to a highly efficient phosphotriesterase with a weak, promiscuous lactonase activity.

The reconstruction of PTEΔ7-2/254R validates the hypothesis that PTE diverged from a yet unknown lactonase and specifically from a quorum-quenching lactonase of the PLL family, and that it could do so within a few mutational events, which is feasible in the time frame of a few decades within which PTE emerged. A nine-amino-acid deletion alongside an adjacent point mutation gave an intermediate that exhibits both the ancestral HSLase activity and the newly diverged paraoxonase activity. PTEΔ7-2/254R exhibits a clear bifunctional character (Table 1, Figure 4): the phosphotriesterase activity is high (k_{cat}/K_M = 5.4 × 10^6 M^{-1} s^{-1}) and just ~17-fold lower than PTE's. Its HSLase activity is only 10–100-fold lower than that of PLL-As for which HSLs are thought to comprise the native substrate. The loose connections between the L7-2 segment and PTE's scaffold and other active-site loops, coupled with the remarkable structural tolerance of this deletion, suggest that the insertion of L7-2 was one of the last steps in PTE's divergence. Thus, as predicted from laboratory evolution experiments,[4] the divergence of a new function (phosphotriesterase, in this case) can proceed a rather long way with weak trade-offs. The ancestral HSLase, activity was only diminished in the very last step(s), upon the insertion of the L7-2 segment that blocked the active-site channel to long chain HSLs (Figure 3b–g), and finally with the R254H mutation. As the specificity of biomeolecules is also shaped by negative selection against certain substrates or ligands, it is possible that the L7-2 insertion in PTE's progenitor was not only driven by the selection for higher paraoxonase activity but also by selection to abolish the HSLase activity.[47] A transposase (tnpA) was identified upstream of the phosphotriesterase gene found in *Agrobacterium radiobacter*.[48] In *Agrobacterium tumefaciens* (which has a phosphotriesterase gene; see Figure 1), HSL-quorum sensing mediated by 3OC8-HSL controls the conjugal transfer of Ti-plasmids.[49] Hence, unlike the PLL progenitor with the L7-2 deletion, PTE that has no HSLase activity would not suppress the transposition that enables its transmission. Although PTEΔ7-2/254R has no detectable activity with 3OC8-HSL, it could may well be that the PLL progenitor that preceded it had this activity (as do many PLL-As).

Ratchet-like mutations, such as R254H, which, unless reverted to their ancestral states, block the effect of key function-altering mutations, were first observed in the divergence trajectory of a glucocorticoid receptors.[46] However, in another case, the reversal of the ancestral function was readily attained with no epistatic effects.[50] In PTE, this ratchet effect is utterly specific to the ancestral HSLase function, whereas the newly evolved PTE activity is hardly affected. However, epistatic, enabling mutations are not unique to reversals and are equally crucial for "forward" trajectories.[22,51,52] Our results also demonstrate the powers of loop remodeling in triggering new enzymatic functions. The reconstruction of the deletion in PTE's loop 7-2 segment resulted in a leap in PTE's HSLase activity with both C4 and 3OC6-HSLs, from undetectable levels in wild-type to k_{cat}/K_M of ~10^4 M^{-1} s^{-1} (Table 1). To our knowledge, activity changes of this order (>10^3-fold) have not been reported for a single backbone change or point mutation. However, in contrast to point mutations that can be readily incorporated by computational or rationale design, and/or directed evolution, the remodeling of active-site loops comprises a challenge.[10,11,14,24−28]

The key to the successful remodeling of PTE's loop 7 has been the assignments of two independent segments of loop 7. However, the alignment mode of two gaps separated by a four-amino-acid "anchor" (Figure 3a) only surfaced after two years of vain attempts to obtain single 14-amino-acid deletion variants. Further, the double gap mode only became visible when new PLLs, especially PLLs that are now dubbed PLL-Bs, were identified[10,12,14] and several crystal structures became available.[10,13,14,16,53,54] However, even with the currently available sequences and structures, all alignment programs we tried except MUSCLE[29] assigned a single gap. But the success in PTE's case may be sporadic. Thus, new computational tools are needed that specialize in loop remodeling as observed in this study, and in a bioinformatics analysis of InDels (insertions and deletions) within a large number of protein families (Toth-Petrozky, Tawfik; in preparation). They may also consider structural parameters such as the degree of solvent exposure, contact density and B-factors, which supported the identification of two individual loop 7 segments and of segment L7-2 as the readily removable one. Another key to the engineering of backbone changes is compensatory and/or enabling mutations. Backbone changes and point mutations seem to be highly correlated (epistatic): the loop L7-2 deletion only confers HSLase activity in conjunction with H254R. Other mutations in sequential and spatial proximity to loop 7 appear to be essential for the acceptance of the deletions of the 7-1 and 7-2 loop segments (see PTEΔ7-1 + 2; Table 1), and variants described in Tables S1 and S2. Such mutations are essential for maintaining the enzyme's configurational stability and/or catalytic activity in the context of backbone changes.

■ ASSOCIATED CONTENT

Supporting Information

A manually refined sequence alignment of PTE from *P. diminuta* and related family members (Figure S1), structural overlay of PTE and PLLs (Figure S2), sequence alignment of PTE and PLLs taken from Afriat et al.[9] (Figure S3), loop 7 superposition of PTE and a PLL-B member (GsP) (Figure S4), PTE's loop 7 conformational flexibility (Figure S5), the oxyanion hole of SsoPox (a PLL-A) and the role of Arg223, the position corresponding to position 254 in PTE (Figure S6), sequence alignment of PTE, its closest PLL homologues, and the predicted most probable ancestral sequences of nodes 9, 12, and 16 (Figure S7). Table S1 describing the ancestral library based on PTEΔ7-2/254R, and Table S2 describes the change in activity and sequence of selected variants from the ancestral library of PTEΔ7-2/254R. This material is available free of charge via the Internet at http://pubs.acs.org.

■ AUTHOR INFORMATION

Corresponding Author

*E-mail: tawfik@weizmann.ac.il. Fax: +972 8 934 4118. Tel: +972 8 934 3637.

Author Contributions

L.A.J. and D.S.T. designed the experiments, performed data analysis, and wrote the manuscript. L.A.J. collected the data. C.J.J. performed structural analysis, assisted in designing the deletion mutants, analyzed data, and participated in writing the manuscript.

Funding

This work was supported by the Defense Threat Reduction Agency (DTRA), by grants from the Willner Albert and Blanche foundation and Jack Wolgin foundation.

Notes

The authors declare no competing financial interest.

■ ACKNOWLEDGMENTS

We are grateful to Mikael Elias for valuable structural and mechanistic insights, Agnes Toth-Petroczy for her help in the alignment construction and structural parameters, and Uria Alcolombri for his help in the ancestral reconstruction.

■ ABBREVIATIONS USED

HSL, homoserine lactone; HSLase, homoserine lactonase activity; InDels, insertions and deletions; OpdA, phosphotriesterase from *Agrobacterium radiobacter*; PLL, phosphotriesterase-like lactonase; PTE, phosphotriesterase from *Pseudomonas diminuta*; TBBL, 5-thiobutyl-γ-butyrolactone

■ REFERENCES

(1) Serdar, C. M., Gibson, D. T., Munnecke, D. M., and Lancaster, J. H. (1982) Plasmid involvement in parathion hydrolysis by *Pseudomonas diminuta*. *Appl. Environ. Microbiol. 44*, 246−249.

(2) Omburo, G. A., Kuo, J. M., Mullins, L. S., and Raushel, F. M. (1992) Characterization of the zinc binding site of bacterial phosphotriesterase. *J. Biol. Chem. 267*, 13278−13283.

(3) Raushel, F. M. H., H. M. (2000) Phosphotriesterase: an enzyme in search of its natural substrate. *Adv. Enzymol. Relat. Areas Mol. Biol. 74*, 51−93.

(4) Khersonsky, O., and Tawfik, D. S. (2010) Enzyme promiscuity: a mechanistic and evolutionary perspective. *Ann. Rev. Biochem. 79*, 471−505.

(5) O'Brien, P. J., and Herschlag, D. (1999) Catalytic promiscuity and the evolution of new enzymatic activities. *Chem. Biol. 6*, R91−R105.

(6) Kikuchi, Y., Hayatsu, M., Hosokawa, T., Nagayama, A., Tago, K., and Fukatsu, T. (2012) Symbiont-mediated insecticide resistance. *Proc. Natl. Acad. Sci. U. S. A. 109*, 8618−8622.

(7) Elias, M., and Tawfik, D. S. (2011) Divergence and convergence in enzyme evolution: Parallel evolution of paraoxonases from quorum-quenching lactonases. *J. Biol. Chem. 287*, 11−20.

(8) Seibert, C. M. R., F. M. (2005) Structural and catalytic diversity within the amidohydrolase superfamily. *Biochemistry*, 6383−6391.

(9) Afriat, L., Roodveldt, C., Manco, G., and Tawfik, D. S. (2006) The latent promiscuity of newly identified microbial lactonases is linked to a recently diverged phosphotriesterase. *Biochemistry 45*, 13677−13686.

(10) Xiang, D. F., Kolb, P., Fedorov, A. A., Meier, M. M., Fedorov, L. V., Nguyen, T. T., Sterner, R., Almo, S. C., Shoichet, B. K., and Raushel, F. M. (2009) Functional annotation and three-dimensional structure of Dr0930 from Deinococcus radiodurans, a close relative of phosphotriesterase in the amidohydrolase superfamily. *Biochemistry 48*, 2237−2247.

(11) Chow, J. Y., Wu, L., and Yew, W. S. (2009) Directed evolution of a quorum-quenching lactonase from Mycobacterium avium subsp. paratuberculosis K-10 in the amidohydrolase superfamily. *Biochemistry 48*, 4344−4353.

(12) Chow, J. Y., Xue, B., Lee, K. H., Tung, A., Wu, L., Robinson, R. C., and Yew, W. S. (2010) Directed evolution of a thermostable quorum-quenching lactonase from the amidohydrolase superfamily. *J. Biol. Chem. 285*, 40911−40920.

(13) Hawwa, R., Aikens, J., Turner, R. J., Santarsiero, B. D., and Mesecar, A. D. (2009) Structural basis for thermostability revealed through the identification and characterization of a highly thermostable phosphotriesterase-like lactonase from *Geobacillus stearothermophilus*. *Arch. Biochem. Biophys. 488*, 109−120.

(14) Hawwa, R., Larsen, S. D., Ratia, K., and Mesecar, A. D. (2009) Structure-based and random mutagenesis approaches increase the organophosphate-degrading activity of a phosphotriesterase homologue from *Deinococcus radiodurans*. *J. Mol. Biol. 393*, 36−57.

(15) Roodveldt, C., and Tawfik, D. S. (2005) Shared promiscuous activities and evolutionary features in various members of the amidohydrolase superfamily. *Biochemistry 44*, 12728−12736.

(16) Elias, M., Dupuy, J., Merone, L., Mandrich, L., Porzio, E., Moniot, S., Rochu, D., Lecomte, C., Rossi, M., Masson, P., Manco, G., and Chabriere, E. (2008) Structural basis for natural lactonase and promiscuous phosphotriesterase activities. *J. Mol. Biol. 379*, 1017−1028.

(17) Dean, A. M., and Thornton, J. W. (2007) Mechanistic approaches to the study of evolution: the functional synthesis. *Nat. Rev. 8*, 675−688.

(18) Bogarad, L. D., and Deem, M. W. (1999) A hierarchical approach to protein molecular evolution. *Proc. Natl. Acad. Sci. U. S. A. 96*, 2591−2595.

(19) Nagano, N., Orengo, C. A., and Thornton, J. M. (2002) One fold with many functions: the evolutionary relationships between TIM barrel families based on their sequences, structures and functions. *J. Mol. Biol. 321*, 741−765.

(20) Voigt, C. A., Martinez, C., Wang, Z. G., Mayo, S. L., and Arnold, F. H. (2002) Protein building blocks preserved by recombination. *Nat. Struct. Biol. 9*, 553−558.

(21) Tawfik, D. S. (2006) Loop grafting and the origins of enzyme species. *Science (New York, N.Y 311*, 475−476.

(22) Ochoa-Leyva, A., Barona-Gomez, F., Saab-Rincon, G., Verdel-Aranda, K., Sanchez, F., and Soberon, X. (2011) Exploring the structure-function loop adaptability of a (beta/alpha)(8)-barrel enzyme through loop swapping and hinge variability. *J. Mol. Biol. 411*, 143−157.

(23) Panchenko, A. R., and Madej, T. (2005) Structural similarity of loops in protein families: toward the understanding of protein evolution. *BMC Evol. Biol. 5*, 10.

(24) Saab-Rincon, G., Olvera, L., Olvera, M., Rudino-Pinera, E., Benites, E., Soberon, X., and Morett, E. (2012) Evolutionary walk between (beta/alpha)(8) barrels: Catalytic migration from triosephosphate isomerase to thiamin phosphate synthase. *J. Mol. Biol. 416*, 255−270.
(25) Park, H. S., Nam, S. H., Lee, J. K., Yoon, C. N., Mannervik, B., Benkovic, S. J., and Kim, H. S. . (2006) Design and evolution of new catalytic activity with an existing protein scaffold. *Science 311*, 535−538.
(26) O'Donoghue, P., Sheppard, K., Nureki, O., and Soll, D. (2011) Rational design of an evolutionary precursor of glutaminyl-tRNA synthetase. *Proc. Natl. Acad. Sci. U. S. A. 108*, 20485−20490.
(27) Murphy, P. M., Bolduc, J. M., Gallaher, J. L., Stoddard, B. L., and Baker, D. (2009) Alteration of enzyme specificity by computational loop remodeling and design. *Proc. Natl. Acad. Sci. U. S. A. 106*, 9215−9220.
(28) Jochens, H., Stiba, K., Savile, C., Fujii, R., Yu, J. G., Gerassenkov, T., Kazlauskas, R. J., and Bornscheuer, U. T. (2009) Converting an esterase into an epoxide hydrolase. *Angew. Chem., Int. Ed. 48*, 3532−3535.
(29) Edgar, R. C. (2004) MUSCLE: multiple sequence alignment with high accuracy and high throughput. *Nucleic Acids Res. 32*, 1792−1797.
(30) Benning, M. M., Shim, H., Raushel, F. M., and Holden, H. M. (2001) High resolution X-ray structures of different metal-substituted forms of phosphotriesterase from *Pseudomonas diminuta*. *Biochemistry 40*, 2712−2722.
(31) Buchbinder, J. L., Stephenson, R. C., Dresser, M. J., Pitera, J. W., Scanlan, T. S., and Fletterick, R. J. (1998) Biochemical characterization and crystallographic structure of an *Escherichia coli* protein from the phosphotriesterase gene family. *Biochemistry 37*, 10860.
(32) Guindon, S., and Gascuel, O. (2003) A simple, fast, and accurate algorithm to estimate large phylogenies by maximum likelihood. *Syste. Biol. 52*, 696−704.
(33) Pupko, T., Pe'er, I., Shamir, R., and Graur, D. (2000) A fast algorithm for joint reconstruction of ancestral amino acid sequences. *Mol. Biol. Evol. 17*, 890−896.
(34) Alcolombri, U., Elias, M., and Tawfik, D. S. (2011) Directed evolution of sulfotransferases and paraoxonases by ancestral libraries. *J. Mol. Biol. 411*, 837−853.
(35) Roodveldt, C., and Tawfik, D. S. (2005) Directed evolution of phosphotriesterase from *Pseudomonas diminuta* for heterologous expression in *Escherichia coli* results in stabilization of the metal-free state. *Protein Eng., Des. Sel. 18*, 51−58.
(36) Herman, A., and Tawfik, D. S. (2007) Incorporating synthetic oligonucleotides via gene reassembly (ISOR): a versatile tool for generating targeted libraries. *Protein Eng. Des. Sel 20*, 219−226.
(37) Jackson, C. J., Foo, J. L., Kim, H. K., Carr, P. D., Liu, J. W., Salem, G., and Ollis, D. L. (2008) In crystallo capture of a Michaelis complex and product-binding modes of a bacterial phosphotriesterase. *J. Mol. Biol. 375*, 1189−1196.
(38) Davies, J. A., Buchman, V. L., Krylova, O., and Ninkina, N. N. (1997) Molecular cloning and expression pattern of rpr-1, a resiniferatoxin-binding, phosphotriesterase-related protein, expressed in rat kidney tubules. *FEBS Lett. 410*, 378−382.
(39) Merone, L., Mandrich, L., Rossi, M., and Manco, G. (2005) A thermostable phosphotriesterase from the archaeon Sulfolobus solfataricus: cloning, overexpression and properties. *Extremophiles 9*, 297−305.
(40) Ng FS, W. D., and Seah, S. Y. (2010) Charateriation of phosphotriesterase-like lactonase from Sulfolobus solfataricus and its immobilization for disruption of quorum sensing. *Appl. Environ. Microbiol. 77*, 1181−1186.
(41) Singh, B. K. (2009) Organophosphorus-degrading bacteria: ecology and industrial applications. *Nat. Rev. Microbiol. 7*, 156−164.
(42) Mulbry, W. W., and Karns, J. S. (1989) Parathion hydrolase specified by the Flavobacterium opd gene: relationship between the gene and protein. *J. Bacteriol. 171*, 6740−6746.
(43) Horne, I., Sutherland, T. D., Harcourt, R. L., Russell, R. J., and Oakeshott, J. G. (2002) Identification of an opd (organophosphate degradation) gene in an Agrobacterium isolate. *Appl. Environ. Microbiol. 68*, 3371−3376.
(44) Dumas, D. P., Caldwell, S. R., Wild, J. R., and Raushel, F. M. (1989) Purification and properties of the phosphotriesterase from *Pseudomonas diminuta*. *J. Biol. Chem. 264*, 19659−19665.
(45) Jackson, C. J., Foo, J. L., Tokuriki, N., Afriat, L., Carr, P. D., Kim, H. K., Schenk, G., Tawfik, D. S., and Ollis, D. L. (2009) Conformational sampling, catalysis, and evolution of the bacterial phosphotriesterase. *Proc. Natl. Acad. Sci. U. S. A. 106*, 21631−21636.
(46) Bridgham, J. T., Ortlund, E. A., and Thornton, J. W. (2009) An epistatic ratchet constrains the direction of glucocorticoid receptor evolution. *Nature 461*, 515−519.
(47) Collins, C. H., Leadbetter, J. R., and Arnold, F. H. (2006) Dual selection enhances the signaling specificity of a variant of the quorum-sensing transcriptional activator LuxR. *Nat. Biotechnol. 24*, 708−712.
(48) Horne, I., Qiu, X., Russell, R. J., and Oakeshott, J. G. (2003) The phosphotriesterase gene opdA in Agrobacterium radiobacter P230 is transposable. *FEMS Microbiol. Lett. 222*, 1−8.
(49) Haudecoeur, E., and Faure, D. (2010) A fine control of quorum-sensing communication in Agrobacterium tumefaciens. *Commun. Integr. Biol. 3*, 84−88.
(50) Huang, R., Hippauf, F., Rohrbeck, D., Haustein, M., Wenke, K., Feike, J., Sorrelle, N., Piechulla, B., and Barkman, T. J. (2012) Enzyme functional evolution through improved catalysis of ancestrally nonpreferred substrates. *Proc. Natl. Acad. Sci. U. S. A. 109*, 2966−2971.
(51) Weinreich, D. M., Delaney, N. F., Depristo, M. A., and Hartl, D. L. (2006) Darwinian evolution can follow only very few mutational paths to fitter proteins. *Science 312*, 111−114.
(52) Povolotskaya, I. S., and Kondrashov, F. A. (2010) Sequence space and the ongoing expansion of the protein universe. *Nature 465*, 922−926.
(53) Gotthard, G., Hiblot, J., Elias, M., and Chabriere, E. (2011) Crystallization and preliminary X-ray diffraction analysis of the hyperthermophilic *Sulfolobus islandicus* lactonase. *Acta Crystallogr. 67*, 354−357.
(54) Zheng, B., Yu, S., Zhang, Y., Feng, Y., and Lou, Z. (2011) Crystallization and preliminary crystallographic analysis of the phosphotriesterase-like lactonase from *Geobacillus kaustophilus*. *Acta Crystallogr. 67*, 794−796.